Table I. Antileukemic Activity of Derivatives of Chrysophanol and Emodin Bearing Alkylating Potential

compd	X	R^1	R^2	R^3	L1210: ID_{50}, μM
5a-I	H	H	Me	Me	128.3
5a-II	H	H	H (or Me)	Me (or H)	11.9
5a-III	H	H	H	H	2.75
6a-I	OH	H	Me	Me	>50
6a-II	OH	H	H (or Me)	Me (or H)	23.4
6a-III	OH	H	H	H	5.92
7a-I	Cl	H	Me	Me	12.5
7a-II	Cl	H	H (or Me)	Me (or H)	1.40
7a-III	Cl	H	H	H	0.13
5b-I	H	OMe	Me	Me	6.91
5b-III	H	OMe	H	H	1.16
6b-I	OH	OMe	Me	Me	>27.6
6b-III	OH	OMe	H	H	13.7
7b-I	Cl	OMe	Me	Me	2.66
7b-II	Cl	OMe	H (or Me)	Me (or H)	1.75
7b-III	Cl	OMe	H	H	0.023
chrysophanol (**1a**)					>393
emodin (1b)					13.3

hypothesis. The presence of both the potent intercalating and alkylating functionalities in the molecule (e.g., **7a,b**-III) maximizes the activity. Lack of one of these functionalities (e.g., **7a,b**-I, which lack potent intercalating capability due to the presence of two bulky methoxy groups, or **1a,b**, which lack the alkylating potential) greatly reduced the cytotoxicity. The activity of 1- or 8-mono-*O*-methylanthraquinones **7a,b**-II falls between that of the 1,8-dihydroxy (7-III) and 1,8-dimethoxy (7-I) analogues. It is also interesting to note that the diethylamino derivatives **5a,b**-III exhibited significant activity whereas the 1,8-di-O-methylated analogues **5a,b**-I showed little cytotoxicity. Due to the presence of basic nitrogen in the molecule, **5a,b**-III can interact more strongly with DNA than the corresponding unmodified natural products, **1a,b**.[9] The 1,8-di-O-methylated derivatives did not interact with DNA most probably due to the presence of two bulky methoxy groups.[9] A very preliminary in vivo test using BDF mice with transplanted L1210/0 leukemia and using a procedure previously described[10] showed that **7a**-III produced an increase in life span of 29% at 25 mg/kg per day × 5.

Studies on the synthesis and biological activities of potential intercalators with alkylating capability are currently under way, and a report on further details will be forthcoming.

(10) A modification of the technique of Fischer (*Ann. N.Y. Acad. Sci.* **1958**, *76*, 673) was employed for cell culture studies. Burchenal, J. H.; Chou, T.-C.; Lokys, L.; Smith, R. S.; Watanabe, K. A.; Su, T.-L.; Fox, J. J. *Cancer Res.* **1982**, *42*, 2598.

† Memorial Sloan-Kettering Cancer Center.
‡ Boston College.

Masao Koyama,† T. Ross Kelly,‡ Kyoichi A. Watanabe*†

Memorial Sloan-Kettering Cancer Center
Sloan-Kettering Division of Graduate School of Medical Sciences
Cornell University
New York, New York 10021
and Department of Chemistry
Boston College
Chestnut Hill, Massachusetts 02167

Received September 14, 1987

Articles

Renin Inhibitors. Design and Synthesis of a New Class of Conformationally Restricted Analogues of Angiotensinogen

Hing L. Sham,* Giorgio Bolis, Herman H. Stein, Stephen W. Fesik, Patrick A. Marcotte, Jacob J. Plattner, Cheryl A. Rempel, and Jonathan Greer*

Pharmaceutical Discovery Division, Abbott Laboratories, Abbott Park, Illinois 60064. *Received June 8, 1987*

Molecular modeling methods have been used to design a novel series of conformationally constrained cyclic peptide inhibitors of human renin. Three goals were defined: enhanced inhibitory potency, high specificity for renin, and increased metabolic stability. Three cyclic compounds were synthesized with ring sizes 10, 12, and 14, based upon a linear hexapeptide inhibitor with a reduced amide replacing the scissile bond at the active site. When tested, the 14-membered-ring compound was as potent an inhibitor of human renin as the parent while the 12-membered-ring compound was 6-fold more potent than the parent against mouse renin. However, the 10-membered-ring compound was inactive against both renins. The lack of potency of the 10-membered compound was explained by using NMR and molecular modeling techniques. It forms another conformation in solution that is inconsistent with binding at the active site. The cyclic compounds did not inhibit either pepsin or cathepsin D significantly. The cyclic modification rendered these inhibitors significantly resistant to cleavage by chymotrypsin and thus prevented loss of activity by this enzyme. Thus, the goals of enhanced inhibitory potency, high specificity, and metabolic stability were achieved in the series of compounds.

The aspartic proteinase renin selectively cleaves the protein substrate angiotensinogen to produce a decapeptide angiotensin I, which is converted by the angiotensin converting enzyme to the potent pressor peptide angiotensin II. Inhibitors of angiotensin converting enzyme have proved to be important modulators of blood pressure.[1,2] Renin inhibitors should exhibit similar antihy-

(1) Cushman, D. W.; Ondetti, M. A. *Prog. Med. Chem.* **1980**, *17*, 41.

0022-2623/88/1831-0284$01.50/0

Scheme I

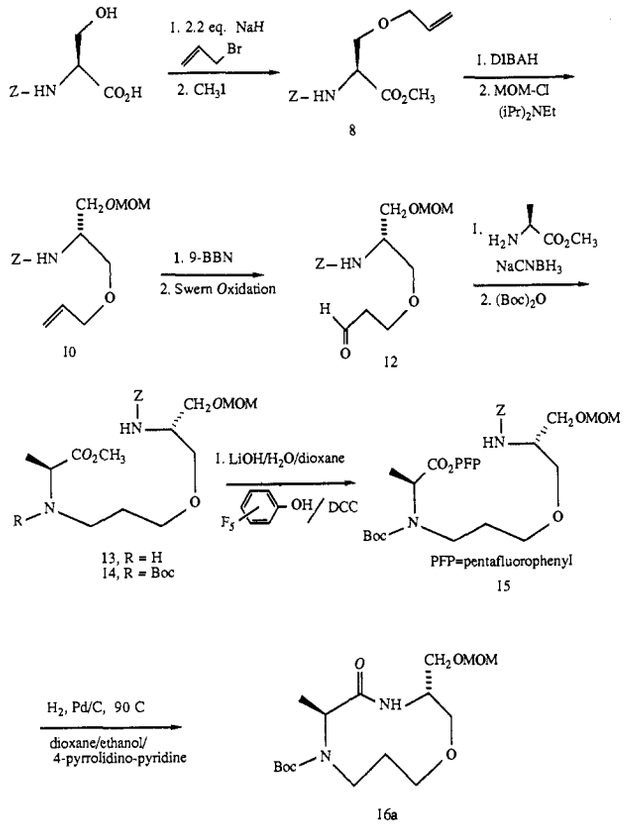

pertensive activity. A number of potent renin inhibitors have been reported[3] that are modifications of the amino acid sequence of angiotensinogen around the site of cleavage by renin. We have been synthesizing a variety of renin inhibitors[4] in which the scissile bond Leu P_1–Val P_1' was replaced by the isosteric reduced amide bond.[5] All the compounds that have been reported are basically peptides which tend to be metabolically unstable and poorly absorbed; none has as yet been found suitable for the clinical treatment of hypertension.

If we wish to depart from a peptide theme for renin inhibitors, it would be very valuable to know the three-dimensional structure of human renin and that of its substrates and inhibitors bound to it. This information is not available from X-ray crystallographic experimental sources.

In the absence of experimental structures, comparative modeling techniques have been used to construct three-dimensional structures for a wide variety of proteins of biological interest from homologous proteins whose structure is known.[6-13] This method has been applied to

Scheme II

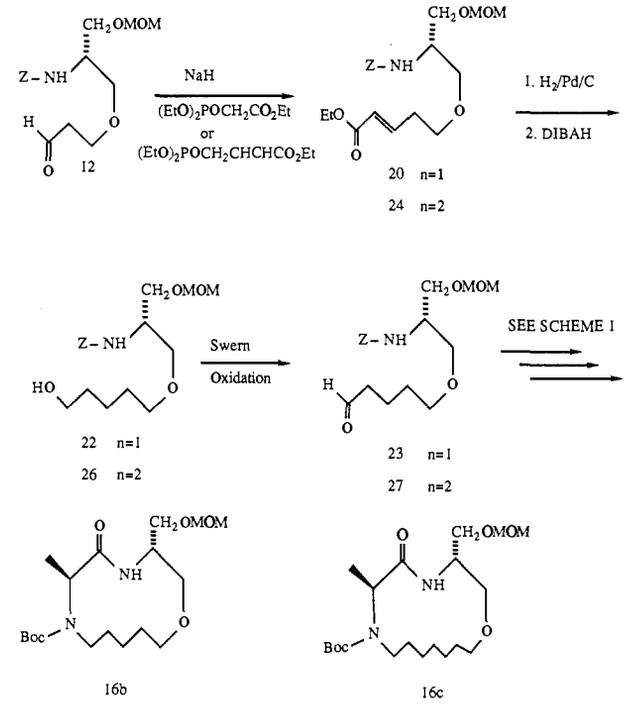

human and mouse renins by a number of groups[14-17] and provides a tentative model structure upon which new renin inhibitors may be designed. Accordingly, we applied comparative modeling methods to produce three-dimensional model structures for human and mouse renin.

Utilizing these model structures, we have designed a series of conformationally restricted peptides. Our particular goals were the following: (i) to achieve at least equipotent binding to renin, (ii) to retain high specificity for renin, and (iii) to increase metabolic stability. In this paper, we report the design and synthesis of a novel series of cyclic peptides with ring sizes 10, 12, and 14. The enzyme inhibition properties are presented and discussed in light of the solution conformation of these compounds and the three-dimensional model structures of renin. The influence on specificity for renin and metabolic stability are also examined.

Chemistry. Schemes I and II give the detailed multistep sequences used to synthesize the cyclic molecules **4–6**.

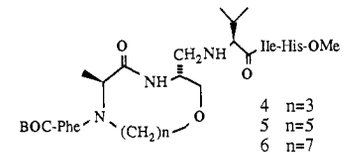

(2) Patchett, A. A.; Harris, E.; Tristram, E. W.; Wyvratt, M. J.; Wu, M. T.; Taub, D.; Peterson, E. R.; Ikeler, T. J.; ten Broeke, J.; Payne, L. G.; Ondeyka, D. L.; Thorsett, E. D.; Greenlee, W. J.; Lohr, N. S.; Hoffsommer, R. D.; Joshua, H.; Ruyle, W. V.; Rothrock, J. W.; Aster, S. D.; Maycock, A. L.; Robinson, F. M.; Hirschmann, R.; Sweet, C. S.; Ulm, E. H.; Gross, D. M.; Vassil, T. C.; Stone, C. A. *Nature (London)* **1980**, *288*, 280.
(3) Boger, J. *Annu. Rep. Med. Chem.* **1985**, *20*, 257.
(4) Plattner, J.; Greer, J.; Fung, A. K.; Stein, H.; Sham, H. L.; Smital, J. R.; Kleinert, H. D.; Perun, T. J. *Biochem. Biophys. Res. Commun.* **1986**, *139*, 982.
(5) Szelke, M.; Leckie, B. J.; Hallett, A.; Jones, D. M.; Sueiras, J.; Atrash, B.; Lever, A. F. *Nature (London)* **1982**, *299*, 555.
(6) Browne, W. J.; North, A. C. T.; Phillips, D. C.; Brew, K.; Vanaman, T. C.; Hill, R. L. *J. Mol. Biol.* **1969**, *42*, 65.
(7) McLachlan, A. D.; Shotton, D. M. *Nature (London) New Biol.* **1971**, *229*, 202.
(8) Greer, J. *Proc. Natl. Acad. Sci. U.S.A.* **1980**, *77*, 3393.
(9) Greer, J. *J. Mol. Biol.* **1981**, *153*, 1027.
(10) Greer, J. *J. Mol. Biol.* **1981**, *153*, 1043.
(11) Greer, J. *Ann. N.Y. Acad. Sci.* **1985**, *439*, 44.
(12) Feldmann, R.; Bing, D. H.; Potter, M.; Mainhart, C.; Furie, B.; Furie, B. C.; Caporale, L. H. *Ann. N.Y. Acad. Sci.* **1985**, *439*, 12.
(13) Greer, J. *Science (Washington, D.C.)* **1985**, *228*, 1055.
(14) Blundell, T.; Sibanda, B. L.; Pearl, L. *Nature (London)* **1983**, *304*, 273.
(15) Sibanda, B. L.; Blundell, T.; Hobart, P. M.; Fogliano, M.; Bindra, J. S.; Dominy, B. W.; Chirgwin, J. M. *FEBS Lett.* **1984**, *174*, 102.
(16) Akahane, K.; Umeyama, H.; Nakagawa, S.; Moriguchi, I.; Hirose, S.; Iizuka, K.; Murakami, K. *Hypertension (Dallas)* **1985**, *7*, 3.
(17) Carlson, W.; Karplus, M.; Haber, E. *Hypertension (Dallas)* **1985**, *7*, 13.

Table I. Percent Identities in the Aspartic Proteinases[a]

	PEN	RHI	END	PEP	REN	HRN
PEN	–	37	59	30	24	21
RHI		–	32	34	26	25
END			–	35	24	22
PEP				–	43	39
REN					–	70
HRN						–

[a] Labels are as follows: PEN, penicillopepsin; RHI, rhizopuspepsin; END, endothiapepsin; PEP, pepsin; REN, mouse renin; HRN, human renin.

Table II. Properties of the Linear and Cyclic Renin Inhibitors

		IC_{50}, μM[a]				NMR conformation		
no.	compound	human renin	mouse renin	porcine pepsin	cathepsin D	% trans	% cis	chymotrypsin cleavage: $t_{1/2}$, min
	P_3 P_2 P_1 P_1' P_2' P_3'							
1	Boc-Phe-His-Leu-$\overset{R}{}$-Val-Ile-His-OMe	0.28	6.5	>10 (10)	>10 (6)	–		–
2	Boc-Phe-Ala-Leu-$\overset{R}{}$-Val-Ile-His-OMe	1.4	0.5	>10 (0)	>10 (0)	100	0	10–15
3	Boc-Phe-Ala-Leu-$\overset{R}{}$-Val-Ile-His-OMe, CH_3	1.2	1.0	>10 (0)	>10 (24)	100	0	–
4	Boc-Phe-Ala-Ser-$\overset{R}{}$-Val-Ile-His-OMe, $(CH_2)_3$	>100 (23)	>100	>10 (0)	>10 (0)	0	100	–
5	Boc-Phe-Ala-Ser-$\overset{R}{}$-Val-Ile-His-OMe, $(CH_2)_5$	69	0.4	>10 (0)	>10 (0)	20	80	–
6	Boc-Phe-Ala-Ser-$\overset{R}{}$-Val-Ile-His-OMe, $(CH_2)_7$	2.7	3.6	>10 (0)	>10 (0)	50	50	not cleaved
7	Iva-Val-Val-Sta-Ala-Sta(pepstatin)	4.6	3.2	0.011	0.046	–	–	–

[a] Numbers in parentheses are the percent inhibition at 10^{-5} M. These are reported when the inhibition was too weak to calculate an IC_{50} value.

The synthetic scheme used to prepare the 10-membered-ring compound **4** is outlined in Scheme I. Treatment of Cbz-L-serine with 2.2 equiv of sodium hydride[18] at 0 °C and sequential addition of allyl bromide (0 °C, 1 h) and then methyl iodide (0 °C→room temperature, 2 h) afforded **8** (75%). Reduction of the methyl ester **8** to the primary alcohol using diisobutylaluminum hydride and protection of the resulting primary alcohol with chloromethyl methyl ether gave compound **10** (80%). Hydroboration of **10** using 9-BBN[19] in THF followed by oxidative workup (H_2O_2/$^-$OH) gave exclusively the primary alcohol (95%), which was oxidized by Swern's method[20] to the corresponding aldehyde **12**. Reductive amination[21] of **12** with alanine methyl ester hydrochloride ($NaCNBH_3$/2-propanol) and sodium acetate as buffer provided the secondary amine **13**, which was protected as the Boc derivative by using di-*tert*-butyl dicarbonate to give compound **14** (72%). The methyl ester in **14** was hydrolyzed at 0 °C by using lithium hydroxide/water/dioxane to give the carboxylic acid (100%). Coupling of the carboxylic acid with pentafluorophenol (DCC/EtOAc) gave the active ester **15** in 97% yield. When **15** was added under high dilution conditions[22-24] to a dioxane solution (~90 °C) containing Pd/C, pyrrolidinopyridine, and ethanol with continuous bubbling of hydrogen through the solution, the cyclic dipeptide equivalent **16a** with a 10-membered ring was formed in 70% yield. The high-resolution mass spectrum of **16a** (calcd, 346.2105; found 346.2105) showed that there was no dimer formation at higher molecular weight. High-field (300 MHz) ^1H NMR of **16a** showed that it was a single diastereomer. No racemization occurred during the high dilution cyclization reaction.

The 12- and 14-membered-ring cyclic dipeptide equivalents **16b** and **16c** were synthesized as shown in Scheme II. Homologation of aldehyde **12** by the Wadsworth and Emmons procedure[25] using sodium hydride and triethyl phosphonoacetate gave **20** (90%). Hydrogenation followed by reduction of the ester to the alcohol gave compound **22** (70%). Swern oxidation of alcohol **22** gave aldehyde **23**. Via the identical sequence of reactions as shown in Scheme I, aldehyde **23** was converted to the 12-membered-ring cyclic dipeptide equivalent **16b** (50% cyclization step). Starting with aldehyde **12** but replacing triethyl phosphonoacetate with triethyl phosphonocrotonate and following the sequence of reactions shown in Scheme I and Scheme II gave the 14-membered-ring cyclic dipeptide equivalent **16c**.

The target compounds **4**, **5**, and **6** were synthesized by the following sequence of reactions using **16a**, **16b**, and **16c** as starting material, respectively: (1) HCl/MeOH; (2) Boc-Phe-NOS/CH_2Cl_2; (3) $(COCl)_2$/DMSO/Et_3N; (4) $NaCNBH_3$/valine benzyl ester hydrochloride/2-propanol/NaOAc; (5) H_2/10% Pd/C; (6) DCC/HOBt/Ile-His-OCH_3·2HCl.

The syntheses of the other molecules presented in Table II have already been described.[5] For synthetic ease, an Ala has been substituted for the naturally occurring His at position P_2 in the inhibitors discussed here. The effect on activity of this substitution is relatively small; a reduction in inhibitory potency of only a factor of 5 (Table II, compare **1** and **2**) was observed.

(18) Sugano, H.; Miyoshi, M. *J. Org. Chem.* **1976**, *41*, 2352.
(19) Brown, H. C.; Rhodes, S. P. *J. Am. Chem. Soc.* **1969**, *91*, 4306.
(20) Omura, K.; Swern, D. *Tetrahedron* **1978**, *34*, 1651.
(21) Borch, R. F.; Hassid, A. I. *J. Org. Chem.* **1972**, *37*, 1673.
(22) Schmidt, U.; Lieberknecht, A.; Griesser, H.; Talbiesky, J. *J. Org. Chem.* **1982**, *47*, 3261.
(23) Schmidt, U.; Lieberknecht, A.; Bokens, H.; Griesser, H. *J. Org. Chem.* **1983**, *48*, 2680.
(24) Schmidt, U.; Lieberknecht, A. *Angew. Chem., Int. Ed. Engl.* **1984**, *23*, 3181.
(25) Wadsworth, W. S., Jr.; Emmons, W. D. *Org. Synth.* **1965**, *45*, 44.

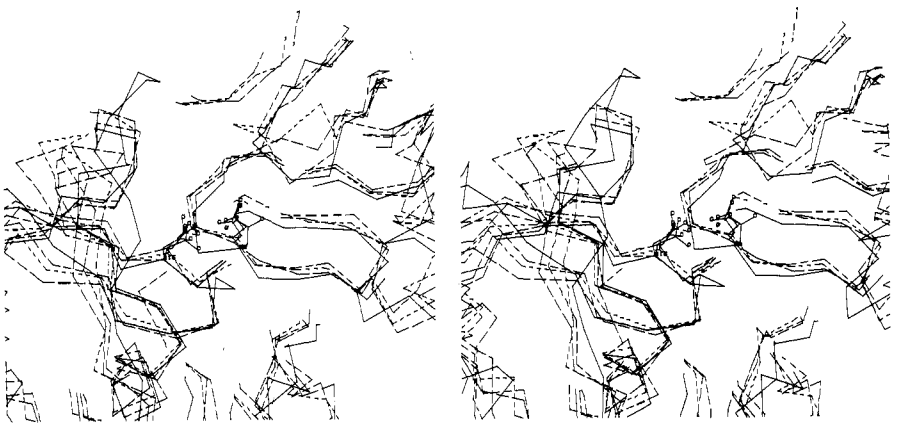

Figure 1. Stereo representation of the active site region of the aspartic proteinases. The four experimentally determined structures are presented: porcine pepsin (solid lines), penicillopepsin (short dashes), rhizopuspepsin (medium dashes), and endothiapepsin (long dashes). The two active aspartates, 32 and 215, are drawn for all four molecules.

Molecular Modeling. A description is presented of the three-dimensional models of human and mouse renin that were used as the structural basis for the design of new renin inhibitors. Major differences between the models used here and those previously described[14-17] are indicated. However, it is beyond the scope of this paper to present a detailed comparison with the previously published models.

The modeling techniques have already been described in detail.[8,9,13] The methods and results differ from previous modeling studies on human and mouse submaxillary gland renin[14-17] because of the inclusion of the porcine pepsin structure.[26] All the experimentally determined three-dimensional structures for aspartic proteinases were assembled, including three fungal enzymes, penicillopepsin,[27] rhizopuspepsin,[28] and endothiapepsin,[29] as well as the mammalian porcine pepsin.[26] The structures were aligned onto each other in three-dimensional space so that their conserved structures were maximized. The overlapped structures show that there are structurally conserved regions (SCRs) among all the four structures and variable regions (VRs) which differ among the known structures. This is comparable to the situation found for the serine proteases.[9] As might be expected, the three fungal enzymes are more closely related while the mammalian pepsin structure differs somewhat from the others.

When the immediate region of the active site of these aspartic proteinases is examined (Figure 1), the structures appear to be more highly conserved than in the rest of the molecule, as expected. Pepsin still differs from the fungal enzymes; however, in some cases, this may be due to the lesser degree of refinement of the pepsin structure than the other fungal proteases.

The sequences, as available, for these proteins were then compiled so that residues that occupied the same positions in the SCRs were aligned (Figure 2). The two renin sequences were then aligned to those of the known structures as follows. As previously described,[8,9,13] the unambiguous sequence homologies that lie in the SCRs were aligned first. Then the rest of the SCRs were aligned without permitting any additions or deletions. Where the length of the SCR differed between the fungal enzymes and pepsin, the shorter SCR extent was used. The remaining portions of the sequence form the VRs. These sections were aligned to the known structure that best fit that sequence in terms of VR length and residue character. The resulting alignment appears in Figure 2.

Table I shows the percent identity between the various sequences of the aspartic proteinases including those of human and mouse submaxillary gland renin, calculated from the alignment in Figure 2. Clearly, the renin sequences are much closer to porcine pepsin than they are to any of the fungal enzymes. A second method of comparing these molecules takes advantage of the variability among related proteins in the nature of their VRs, where all the additions and deletions typically occur.[9] Because the SCRs differ in size between the fungal enzymes and pepsin (Figure 2), a simple straightforward comparison of all the VRs among the species is not possible. However, it is clear that in this respect the renins are also much more closely related to pepsin. For the VRs around residues 196–210 and 286–300, as well as for the long region from 252–283 where the pepsin structure differs from the fungal enzymes, sequence length and homology show a closer relationship of the renins to pepsin than to the fungal proteases. The above considerations suggest that the pepsin structure should be weighted more heavily in the modeling process. However, since the pepsin structure has not been as fully refined as the other aspartic proteinase structures, it probably should not be used exclusively.

Using this sequence alignment for the renins, we constructed the three-dimensional models. In general, the main chain coordinates for the SCRs were taken from the pepsin structure, with the exception of the immediate active site area, which was taken from the better refined penicillopepsin structure. This consisted of residues 30–38 and 210–222, including the two active site aspartates, 32 and 215.

The value of including the pepsin structure in the modeling is illustrated by the close relationship between the renin sequences and pepsin in two of the VRs that lie in the immediate region about the active site and certainly interact with substrates and inhibitors. One, which lies at positions 70–80, is known as the flap because, presumably, it must move to allow the substrate or inhibitor to bind and then folds down over the substrate or inhibitor to interact with it. It has been shown to interact with inhibitors in the crystal and to change its conformation upon such binding.[33,34] The flap has very different lengths

(26) Andreeva, N. S.; Zdanov, A. S.; Gustchina, A. E.; Fedorov, A. A. *J. Biol. Chem.* **1984**, *259*, 11353.
(27) James, M. N. G.; Sielecki, A. R. *J. Mol. Biol.* **1983**, *163*, 299.
(28) Bott, R.; Subramanian, E.; Davies, D. R. *Biochemistry* **1982**, *21*, 6956.
(29) Pearl, L.; Blundell, T. *FEBS Lett.* **1984**, *174*, 96.
(30) Misono, K. S.; Chang, J.-J.; Inagami, T. *Proc. Natl. Acad. Sci. U.S.A.* **1982**, *79*, 4858.

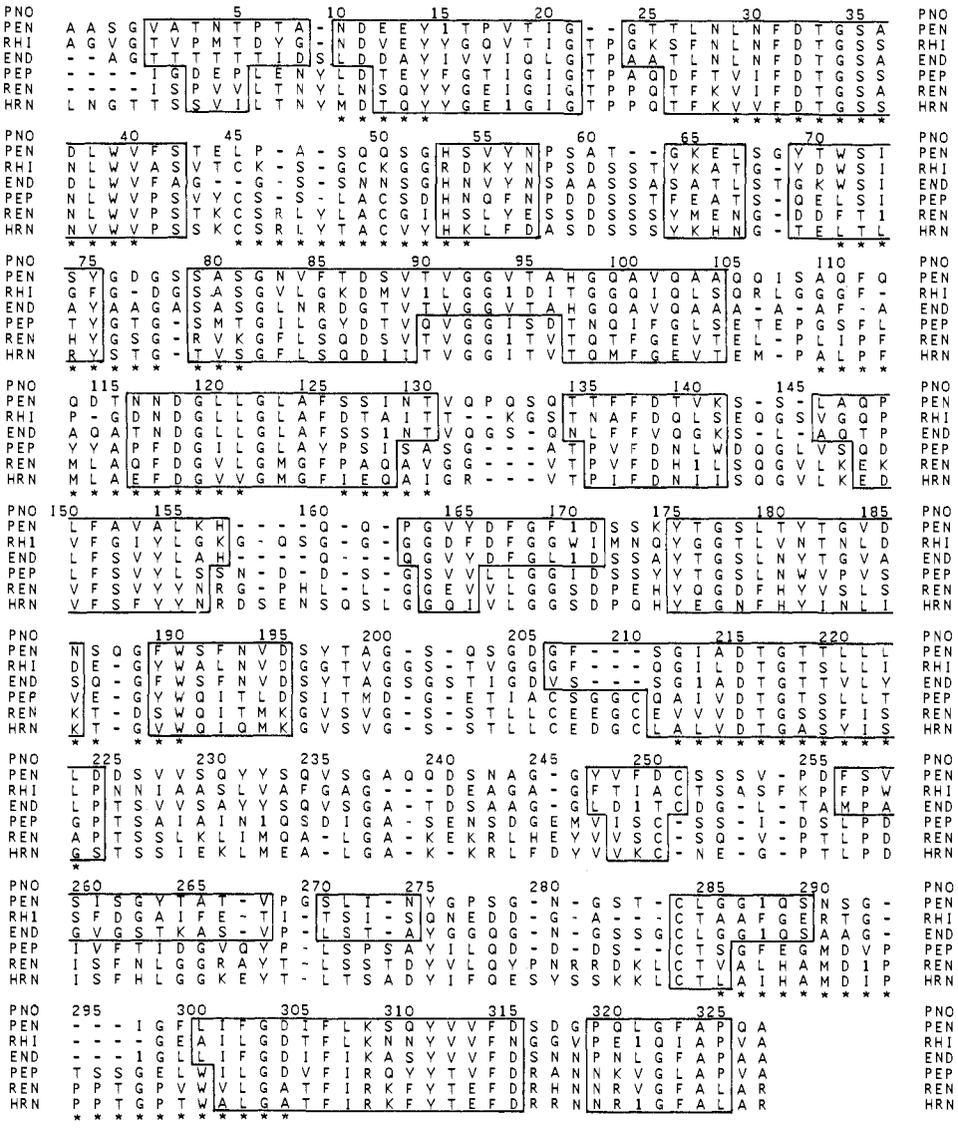

Figure 2. Sequence alignment for the four structurally determined aspartic proteinases: penicillopepsin (PEN), rhizopuspepsin (RHI), endothiapepsin (END), and porcine pepsin (PEP). This alignment is based upon the correspondence of the three-dimensional structures. The pepsin numbering is included at the top for reference (PNO). This numbering is used for all aspartic proteinases in this paper. The SCRs for these proteins are enclosed in boxes. The two renin sequences, mouse (REN) and human (HRN), have been aligned to the other aspartic proteinases as described in the text. The asterisks under the human renin sequence denote those residues in the immediate active site included in the energy calculations. The sequences for the fungal enzymes and pepsin were taken from the reported X-ray structures.[26-29] Mouse submaxillary gland renin was from Misono et al.[30] and human renin from Imai et al.[31] and Soubrier et al.[32] Residues are represented by the single letter code following the IUPAC–IUB convention: A = Ala, C = Cys, D = Asp, E = Glu, F = Phe, G = Gly, H = His, I = Ile, K = Lys, L = Leu, M = Met, N = Asn, P = Pro, Q = Gln, R = Arg, S = Ser, T = Thr, V = Val, W = Trp, Y = Tyr.

and conformations in the known aspartic proteinases (Figures 1 and 2); however, the renin and pepsin molecules have the same length flap and very similar residue types in the flap.

The second VR consists of residues 295–300. This loop is four to five residues shorter in all three fungal enzymes (Figures 1 and 2). In pepsin, the loop is the same length as in the renin sequences and there is even some sequence homology. However, the occurrence of a relatively unique Pro-Pro-Pro sequence in both human and mouse renins indicates that while the pepsin conformation of this loop was a more useful guide than the fungal enzymes, it had to be modified to accommodate the renin sequence. For this purpose, all the known structures in the Brookhaven protein data bank[35] were examined for similar Pro-Pro-Pro sequences. Such stretches of Pro's were found in several proteins (guinea pig IgG1, 1PFC in the Brookhaven data base; and phosphoglycerate mutase, 3PGM[35]), which were then used to guide the modeling of this loop. The residues were constructed to the Pro-Pro-Pro conformations in these proteins and then modified minimally to fit onto the ends of this loop in the renin structure. Since both the flap and the Pro-Pro-Pro loop form an integral part of the active site binding region, the conformations that have

(31) Imai, T.; Miyazaki, H.; Hirose, S.; Hori, H.; Hayashi, T.; Kageyama, R.; Ohkubo, H.; Nakanishi, S.; Murakami, K. *Proc. Natl. Acad. Sci. U.S.A.* **1983**, *80*, 7405.
(32) Soubrier, F.; Panthier, J.-J.; Corvol, P.; Rougeon, F. *Nucleic Acids Res.* **1983**, *11*, 7181.
(33) James, M. N. G.; Sielecki, A.; Salituro, F.; Rich, D. H.; Hofmann, T. *Proc. Natl. Acad. Sci. U.S.A.* **1982**, *79*, 6137.
(34) James, M. N. G.; Sielecki, A. R. *Biochemistry* **1985**, *24*, 3701.
(35) Bernstein, F. C.; Koetzle, T. F.; Williams, G. J. B.; Meyer, E. F., Jr.; Brice, M. D.; Rodgers, J. R.; Kennard, O.; Shimanouchi, T.; Tasumi, M. *J. Mol. Biol.* **1977**, *112*, 535.

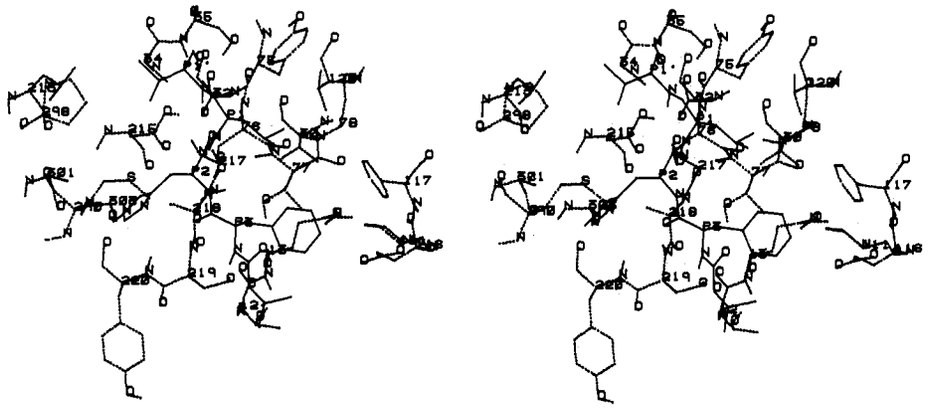

Figure 3. Stereo representation of the energy minimized active site of human renin (dotted lines) with the parent hexapeptide inhibitor 1 bound (solid lines). The renin residues are labeled with the pepsin numbering system (Figure 2), and the inhibitor residues are denoted by P_3, P_2, ..., etc.[36] The minimizations were performed with all hydrogens. However, for clarity, in this and in the next figure, only the polar hydrogens are shown. Note the apparent open area between the side chain of Leu P_1 and the main chain NH of His P_2.

been selected are crucial to the detailed understanding of substrate and inhibitor binding to renin.

A tentative model for the renin enzyme having been produced, the next step was to model the interaction between a substrate or inhibitor and the enzyme. Two experimental crystal structures are available: a complex of pepstatin with the rhizopus enzyme[28] and a pepstatin fragment on the penicillopepsin molecule.[33,34] The parent inhibitor chosen for the renin inhibitor modeling was the hexapeptide 1 (Table II), Boc-Phe-His-Leu^{R}Val-Ile-His-OMe. The crystal enzyme-inhibitor structures clearly indicate the interactions between the portion of the inhibitor N-terminal to the scissile bond, Boc-Phe-His-Leu (P_3–P_1),[36] and the enzyme; thus, the main chain coordinates for this part of the inhibitor were used directly and the angiotensinogen sequence "mutated" onto this main chain. However, the unusual main chain of the statine residue does not provide a direct model of the C-terminal portion of the inhibitor, Val-Ile-His-OMe (P_1'–P_3'). This portion was modeled by exploring all possible conformations for the Val-Ile-His-OMe on the enzyme surface that were similar to the binding conformation of the pepstatin molecule.[37] One unique conformation was found for the Val P_1' and Ile P_2' positions. However, for His P_3', several possible conformations were accessible; no interactions were found for the OMe moiety.

In order to maximize the reliability of the renin modeling and its implications for drug design, the decision was made to restrict further analysis of the model structure to the active site region. This is advantageous because the four experimental structures are so similar in this area, making the modeling most reliable. The structures of the aspartic proteinases diverge increasingly the greater the distance from the active site. The active site region was defined as all residues that lay within 7 Å of any atom on the hexapeptide inhibitor 1. Additional residues were added to complete a disulfide bridge loop around residues 45 and 52. This region had been constructed from an optimal combination of the penicillopepsin and pepsin structures (see above). The resulting active site contained nine fragments of the renin molecule; the residues included are noted in Figure 2.

This model renin active site with inhibitor 1 bound was modified by hand to remove bad inter-side-chain contacts by rotating about the respective side chain χ angles. The N- and C-terminal residues of each fragment, which lay outside the 7-Å volume, were kept fixed during the minimization in order to avoid any significant departures from the model because the rest of the protein was not included. Because of the close proximity of Asp 32 and Asp 215 and current proposals for aspartic proteinase mechanism of action,[3,29,34] Asp 215 was protonated for the energy calculations. The total structure that was minimized, including the inhibitor, consisted of 1650 atoms.

Energy minimization was performed by using the program VFFPRG of Dr. A. T. Hagler and co-workers.[39,40] In the first step, consisting of 200–300 cycles, every atom of the system was constrained with a forcing potential to remain in close proximity to the starting structure. This technique allows relaxation of close contacts without introducing drastic distortions into the structure. In the second step, the system was allowed to relax (the terminal residues of each fragment being held fixed). A typical minimization required 2500–3000 iterations to bring the system to a stable minimization defined by the maximum derivative of the potential function ≤ 0.01. This required about 30 h of computing time on a FPS-164 array processor. A number of linear peptides were minimized in the active site, and the resulting structures were used for designing new inhibitors.

Calculations were performed for the cyclic inhibitors by using the same active site (Figure 2). Care was taken to avoid close contacts between the inhibitor and the enzyme in each case by manipulating the conformation of the macrocycles. The final minimized structures were compared to see what the effects were of the respective inhibitor on the enzyme and inhibitor structures.

Results

Modeling the Cyclic Structures. The three-dimensional model structure for the hexapeptide inhibitor 1 bound to the active site of human renin, together with some of the catalytically important residues, is shown in Figure 3. The model suggests a variety of modifications that might restrict the conformational space of the inhibitor. In particular, the side chain of residue P_1 lies in reasonable proximity to the main chain NH of residue P_2

(36) Schechter, I.; Berger, A. *Biochem. Biophys. Res. Commun.* **1967**, *27*, 162.
(37) Boger, J. In *Peptides: Structure and Function, Proceedings of the 8th American Peptide Symposium*; Hruby, V. J., Rich, D. H., Eds.; Pierce Chemical: Rockford, Il, 1983; pp 569–578.
(38) Reference deleted in press.
(39) Hagler, A. T.; Stern, P. S.; Sharon, R.; Becker, J. M.; Naider, F. *J. Am. Chem. Soc.* **1979**, *101*, 6842.
(40) Dauber, P.; Osguthorpe, D.; Hagler, A. T. *Biochem. Soc. Trans.* **1972**, *10*, 312.

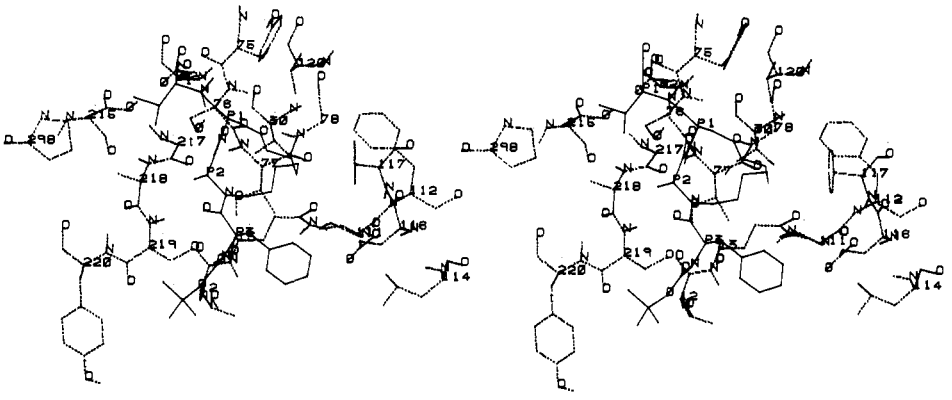

Figure 4. Stereo representation of the energy minimized structure of the 14-membered cyclic renin inhibitor **6** (solid lines) bound to the active site of human renin (dotted lines). The residues are labeled as in Figure 3. The introduction of the bridge between the side chain of P_1 and the main chain NH of P_2 causes a shift in the flexible flap around residues 77–79, which move up to 2.5 Å. See the description in the text.

to permit these two groups to be bridged. Because, in a model structure such as that of renin and the bound inhibitor, the three-dimensional coordinates are not exact, the strategy was adopted of designing a series of such molecules.

The cyclic molecules shown in Table II, **4–6**, were designed to bridge from a simple side chain at position P_1 to the NH at P_2 via three through seven methylene units. Each structure was constructed in the computer, placed in the active site of renin, and minimized in order to see whether the bridge perturbed the conformation of the inhibitor, or of the enzyme, or prevented any important interactions in the complex (Figure 4). The only significant changes to the structure occurred in the loop of residues from 70 to 80 that lies directly on top of the substrate or inhibitor.[28,33,34] It is called the "flap" because it changes its conformation to interact with substrates or inhibitors when they bind to the enzyme.[33,34] Residues 77 through 79 moved up to 2.5 Å in order to make room for the methylenes that bind to the main chain NH of position P_2; the displacement of the flap was less in the 10-membered-ring compound than in the 14-membered-ring compound. However, the specific interactions that occur between the flap and the inhibitor, such as the H bond between Ser 76 of the flap and the main chain carbonyl of position P_2, remained. The main chain of the cyclic inhibitors did not deviate significantly from the main chain of the parent compound; thus, it retained all the important binding interactions with the rest of the enzyme.

Inhibitory Activity of the Cyclic Inhibitors. In order to test the validity of the model in the region of residues P_2 and P_1 and the feasibility of this bridging design, a linear inhibitor, **3**, was synthesized with the NH at position P_2 methylated in order to insure that substitution at this site did not destroy activity. This compound was equipotent to the parent **2**.

The 10-, 12-, and 14-membered cyclic compounds, **4**, **5**, and **6**, respectively, were synthesized as described in the Experimental Section. Their ability to inhibit human and mouse renins was measured and is summarized in Table II. For human renin, the 10-membered-ring compound **4** was a poor inhibitor, the 12-membered-ring compound **5** was better, and the 14-membered-ring compound **6** was a little less potent than the corresponding Ala-containing peptide, **2** or **3**. The results for mouse renin were even more interesting. The 10-membered-ring **4** was again inactive; however, the 12-membered-ring inhibitor **5** was more than twice as potent as the parent peptide **3**, and the 14-membered-ring **6** was a little weaker than the parent compound.

The cyclic compounds were tested for inhibition of other aspartic proteinases. None of the cyclic compounds showed inhibition of either pepsin or cathepsin D at 10^{-5} M. For comparison, the standard aspartic proteinase inhibitor, pepstatin **7**, was at least 3 orders of magnitude more potent an inhibitor of pepsin and cathepsin D (Table II).

Structural Studies on the Cyclic Inhibitors. NMR methods were used to determine the conformational properties of the 10-, 12-, and 14-membered cyclic peptides in solution. Two sets of resonances were observed in the ^{1}H NMR spectra of these peptides, despite extensive purification by HPLC. For example, in the ^{1}H NMR spectrum of the 14-membered-ring peptide, Ala P_2 methyl proton signals appear both at their "normal" location (1.4 ppm) and upfield at 0.6 ppm. When the upfield alanine methyl resonance was irradiated in a saturation transfer experiment,[41] a decrease in the intensity of the Ala methyl resonance at 1.4 ppm was observed. These results indicated that the two sets of resonances corresponded to two interconverting conformation states for the 14-membered-ring inhibitor. This conclusion is consistent with the observed coalescence of the two sets of resonances at higher temperature. From the coalescence temperature (~110 °C) of the Ala methyl protons of the 14-membered cyclic peptide in DMSO-d_6, an energy activation barrier of ~18 kcal/mol was calculated[42] for the interconversion between the two states.

The magnitude of the activation energy could be explained by a cis/trans isomerization of the peptide bond of an N-substituted amino acid.[43,44] The presence of a cis peptide bond between Phe P_3 and Ala P_2 was confirmed in the 10-membered-ring compound **4** by a strong nuclear Overhauser effect (NOE) between the α-protons of the Phe and Ala residues in a two-dimensional NOE experiment. Further NOEs that were observed between the Ala methyl protons and the Phe aromatic protons, as well as the upfield shift of the Ala methyl protons, were all consistent with a cis Phe–Ala peptide bond.[45]

The NMR spectra for the peptides were analyzed in detail to determine the fraction of each compound in the cis and trans states (Table II). The proportion of cis to

(41) Forsén, S. H.; Hoffman, R. A. *J. Chem. Phys.* **1963**, *39*, 2892.
(42) Sandström, J. *Dynamic NMR Spectroscopy*; Academic: New York, 1982; 96.
(43) Stewart, W. E.; Siddall, T. H. *Chem. Rev.* **1970**, *70*, 517.
(44) Wüthrich, K.; Grathwohl, C. *FEBS Lett.* **1974**, *43*, 337.
(45) Fesik S. W.; Bolis, G.; Sham, H. L.; Olejniczak, E. T. *Biochemistry* **1987**, *26*, 1851.

trans varied among the cyclic peptides, with the 10-membered-ring **4** being all cis, the 12-membered cyclic **5** being 80% cis, and the 14-membered-ring **6** being approximately 50% cis, 50% trans.

Chymotrypsin Cleavage. Upon incubation of the parent compound **2** with a commercial preparation of chymotrypsin, rapid cleavage of the Phe–Ala bond was observed. At the same time, the C-terminal methyl ester is hydrolyzed, resulting in the major products at completion being Boc-Phe and Ala-Leu^{R}Val-Ile-His. Both reactions exhibited half-times of 10–15 min under our conditions and proceeded to near completion in a 1-h incubation. In contrast, the cyclic compound **6** was not susceptible to cleavage at the Phe–Ala bond, but was cleanly converted to the carboxylic acid ($t_{1/2} \sim 10$ min) upon incubation with the same enzyme preparation (Table II).

Discussion

Molecular modeling methods have been utilized to rationally design a new series of conformationally restricted cyclic peptide renin inhibitors. In designing cyclic molecules in a hexapeptide such as **2**, a large number of bridges are possible in principle between the many groups in the molecule. A great advantage of having a three-dimensional model for the inhibitor and for the inhibitor–enzyme complex is that many of these possibilities can be eliminated either as conflicting with the desired binding conformation of the inhibitor or as colliding with some important part of the enzyme binding pocket. More importantly, the model can be used to identify reasonable candidates for bridging because of their proximity that would never be chosen if such a three-dimensional model did not exist. Using the model, we selected two such specific groups, the side chain at position P_1 and the main chain NH of position P_2, because of their closeness and then linked them by a synthetically accessible methylene bridge. Different-length bridges were examined, and a series was chosen that was consistent with the model and with energy calculations.

The chosen molecules were synthesized and tested in human and mouse renin, which differ somewhat in the residues of the active site region, especially in the flap (Figure 2). The 14-membered-ring compound was found to be half as potent as the *N*-methyl Ala parent, **3**, in inhibiting human renin while the 12-membered-ring compound was twice as potent against mouse renin. These results are highly significant because of the major changes in structure that were introduced into these inhibitors. One of the most important side chains, Leu P_1, was modified. The main chain itself of His P_2 was derivatized at the NH. A methylene bridge was introduced to connect these two groups. Furthermore, such a bridge drastically constrains the possible conformations that the P_1–P_3 region of the inhibitor can adopt. These changes were introduced because the renin–inhibitor complex model suggested that they could be accommodated without loss of activity. The fact that the 12- and 14-membered-ring compounds were determined to be equal or more potent inhibitors of renin demonstrates and supports the validity of the renin models and their value for prediction in the important P_1–P_3 region of the structure. In particular, we have shown that the main chain NH of His P_2 can be modified with little or no loss of activity as predicted by the model. A methylene bridge can be added between Leu P_1 and His P_2 NH causing restriction of the P_1–P_3 conformation, and at least equipotent activity is obtained as anticipated from the model structure.

Nevertheless, from the perspective of improving our ability to do drug design and modeling, we were puzzled as to why the 10-membered-ring compound was inactive, since it also seemed to fit into the renin model active site satisfactorily. Consequently, we decided to analyze the structural properties of the cyclic inhibitors in solution.

Detailed structural analyses by NMR of the cyclic compounds substituted at the main chain N of Ala P_2 have shown that the Phe P_3–Ala P_2 peptide bond exists as cis and trans isomers. Cis peptide bonds are stabilized when the main chain NH is substituted, as is found for proline.[44] Examination of the model structure for the inhibitor–renin complex indicates that the cis form of the inhibitor cannot fit into the active site of renin. Major collisions occur between the Boc and Phe P_3 of the inhibitor and residues 217 through 219 of renin (Figures 3 and 4). It appears that only the trans form can bind to the enzyme.

This discovery of an inactive cis form of the inhibitors allows the complete rationalization of the inhibition of human renin by the cyclic compounds. The 10-membered ring is inactive because it is entirely cis. The 12-membered ring shows a little activity since it is partially in the trans form. Very significant activity is found for the 14-membered ring since it is 50% in the trans form. When corrected for being only 50% in the active form, the 14-membered ring is just as active as the unsubstituted parent molecule, **2** (Table II).

This simple correlation is not sufficient to explain the inhibition results for mouse renin by these cyclic compounds (Table II). Now the 12-membered ring, **5** is 10-fold better than the 14-membered ring, **6**, even though it is 80% cis versus 50% cis. The interpretation of the mouse renin results requires the introduction of another effect. A possible explanation is offered from modeling considerations. Modeling of the cyclic compounds on the active site of both human and mouse renin shows that the larger ring compounds are filling the Leu P_1 site in much the same way that cyclohexylalanine fills the Leu side chain pocket and improves the inhibitory potency.[46] This effect acts together with the increased amount of trans isomer to improve the inhibitory properties of the cyclic molecules in human renin as the size of the cycle increases. In mouse renin, however, the active site appears to have a little smaller P_1 pocket than does human renin. Thus, maximum inhibition is achieved with the 12-membered ring, **5**, where a significant amount of the trans isomer is present and presumably the ring just fills the Leu P_1 pocket in mouse renin. In the 14-membered-ring compound, there is more trans isomer; however, the ring is now just too large for the pocket in mouse renin and, consequently, the inhibitory potency drops 9-fold (or about 22-fold if the proportion of trans isomer is taken into account).

There is corroboratory experimental evidence that the mouse renin Leu P_1 pocket does not accommodate larger side chains as well as human renin. This is demonstrated by the decreased enhancement of cyclohexylalanine versus leucine at position P_1 of the inhibitor in mouse versus human renin.[46] For the compound reported in that reference, the enhancement ratio for human renin was 55–76, while for mouse it was only 7. In four series of compounds that we have examined (details to be published elsewhere), the average enhancement ratio for cyclohexylalanine versus leucine at position P_1 was 21 in human renin while for mouse renin it was only 3.

There were three goals defined for the design of cyclic renin inhibitors from rational molecular modeling sources.

(46) Boger, J.; Payne, L. S.; Perlow, D. S.; Lohr, N. S.; Poe, M.; Blaine, E. H.; Ulm, E. H.; Schorn, T. W.; LaMont, B. I.; Lin, T.-Y.; Kawai, M.; Rich, D. H.; Veber, D. F. *J. Med. Chem.* **1985**, *28*, 1779.

How well have these goals been met? The first was to achieve at least equipotent renin inhibition. A conformationally constrained molecule should, if all other interactions with the enzyme and solvent remain the same, be a more potent inhibitor than the parent molecule because the entropy loss due to conformation restriction upon binding to the enzyme should be diminished. For an inhibitor that is so enveloped by the enzyme as are the renin inhibitors (Figures 3 and 4), it is difficult to modify the inhibitor around P_1–P_3 without affecting some interaction with the enzyme in the active site region. Nevertheless, using the model structure for renin, we attempted to design a cyclic series that perturbed the active site and the important inhibitor–enzyme interactions as little as possible in order to maximize inhibitory potency. It is a considerable success that the significantly modified inhibitors proposed in this work have turned out to be equipotent to and more potent than the parent. Indeed, when the factors for the presence of the inactive cis conformation forms are taken into account (Table II), then the 14-membered **6** is fully as potent as the parent linear peptide containing Ala P_2, **2**, on human rein. In mouse renin, when the proportion of trans isomer is included, the 12-membered ring, **5**, is 6-fold more potent than the parent linear Ala P_2 peptide **2**. Thus, enhanced binding has indeed been attained.

The second goal of high specificity for renin has been achieved by these compounds as seen in Table II. They demonstrate no detectable inhibition of the other aspartic proteinases pepsin or cathepsin D at 10^{-5} M. Thus, the high specificity of the parent compounds for renin has been preserved in the cyclic inhibitors.

The last goal was to achieve increased stability of the inhibitor to enzymatic degradation. This goal is crucially important for the design of orally active agents. When the parent linear renin inhibitors were treated with a number of tissue homogenates, the major activity that degraded them was due to the intestinal protease chymotrypsin (P. Marcotte, unpublished results). Thus, linear peptide inhibitors of renin such as **2** are rapidly cleaved by chymotrypsin (Table II) at the peptide following Phe P_3, completely destroying renin inhibitory activity. Similar digestion studies on the cyclic molecule **6** showed it to be very significantly more stable at this bond than the linear parent compounds.

The relatively modest potency of the cyclic inhibitors by current standards[46] precludes the development of these compounds as therapeutic agents. However, the goals of enhanced inhibition, high specificity, and significantly increased metabolic stability have been achieved in this series of cyclic peptides based upon rational drug design. The results reported here and their interpretation illustrate the success but also the complexity of rationally designing new inhibitor compounds. Some of the important factors in the design strategy have been discussed and illustrated. The important lesson has been demonstrated vividly that new solution conformations of the inhibitors may become stable which were not expected at the outset. More effort needs to be expended to try to discover such potentially unproductive conformations during the design process. As more experience is gathered in the relatively young field of rational drug design by molecular modeling, it is hoped that many of these problems can be anticipated and avoided and that potent, therapeutically useful molecules will result.

Experimental Section

Renin Assay. The compounds were dissolved in DMSO and diluted so that prior to addition to the assay system the solutions were 10% in DMSO and 0.5% in BSA. For the human enzyme, the final incubation mixture (100 μL) contained maleate buffer, pH 6.0, 0.135 M; EDTA, 3mM; PMSF, 1.4 mM; pure human angiotensinogen,[47] 0.21 μM; purified human renal renin,[48] 0.24 mGU;[49] BSA, 0.44%; and DMSO, 1%. The mouse renin assay contained the same maleate, EDTA, PMSF, BSA, and DMSO concentrations, plus 3.45 mM 8-hydroxyquinoline; the enzyme was 20 ng of purified protein.[50] Dog plasma diluted 1.5:10 served as the substrate. At least three different concentrations of inhibitor, bracketing the expected IC_{50}, were preincubated with renin for 5.0 min at 37 °C, substrate was added, and the incubation was allowed to proceed for 10.0 min. The reaction was stopped by freezing the solution in a methanol/dry ice bath, and after thawing at 4 °C, an aliquot was analyzed for angiotensin I by radioimmunoassay (New England Nuclear). The percent inhibition of the renin reaction at a given inhibitor concentration causing 50% inhibition was calculated by regression analysis. Confidence limits, determined by means of Fieller's theorem,[51] were within ±20% at the 95% level. The reaction time of 10 min was on the linear portion of the incubation time–angiotensin I generation curve, and at the highest concentrations tested, none of the compounds cross-reacted with the antibody to angiotensin I. The presence of 1% DMSO in the final incubation mixture exerted no statistically significant effect on the activity of renin.

Pepsin and Cathepsin D Assays. Porcine pepsin (Sigma) and bovine cathepsin D (Sigma) activities were assessed by the hydrolysis of hemoglobin at pH 1.9 and 3.1, respectively, at 37 °C, and measurement of the absorbance at 280 nm of the supernatant after precipitation with trichloroacetic acid.[52]

Chymotrypsin Cleavage Experiment. Stock solutions of the respective renin inhibitor were dissolved at 5 mg/mL in methanol. A 50-μL aliquot of this solution was then diluted into 2450 μL of 30 mM sodium phosphate/100 mM sodium chloride, pH 6.9, containing 10 μg/mL bovine chymotrypsin (Sigma C 4129) and incubated at 37 °C (0.1 mg/mL final concentration of compound). At intervals, 100-μL aliquots were removed, acetonitrile was added to 10%, and the composition was analyzed by injection onto a Waters μBondapak C-18 analytical HPLC column eluted with a gradient from 12.5% to 65% acetonitrile and equilibrated throughout with 0.1% in trifluoroacetic acid. A single-wavelength UV monitor (214 nm) was employed for detection, and quantitation was achieved by using a Perkin-Elmer LCI-100 computing integrator.

Analytical. Proton nuclear magnetic resonance spectra were recorded at 60 MHz with a Varian Model EM360 instrument and at 300 MHz with a Nicolet 300 Fourier transform spectrometer. Chemical shifts were reported as δ units (ppm) relative to tetramethylsilane as internal standard. TLC was performed on 0.25-mm thickness silica gel plates (Merck; silica gel 60F–254). For flash column chromatography and medium-pressure liquid chromatography (MPLC), Merck silica gel, grade 60, 230–400 mesh, was used.

NMR Methods. Samples for conformational analysis were prepared in 5-mm NMR tubes by dissolving 2–12 mg of the peptides in $CDCl_3$, DMSO-d_6, or DMSO-d_6/D_2O (66:34). ^1H NMR spectra were recorded on a Nicolet NT-360 NMR spectrometer, operating at a frequency of 361.1 MHz. Saturation transfer experiments[41] were performed by subtracting the free induction decays (FID) acquired with preirradiation (0.5 s) at the frequency of interest from the control FID accumulated with preirradiation where no signals are present. Pure absorption phase 2D NOE data sets were acquired by using a $(90°–t_1–90°–\tau_m–90°–\text{acquire})_n$

(47) Dorer, F. E.; Lentz, K. E.; Kahn, J. R.; Levine, M.; Skeggs, L. T. *Anal. Biochem.* **1978**, *87*, 11.
(48) Stein, H. H.; Fung, A. K. L.; Cohen, J. *Fed. Proc., Fed. Am. Soc. Exp. Biol.* **1985**, *44*, 1363.
(49) Bangham, D. R.; Robertson, I.; Robertson, J. I.; Robinson, C. J.; Tree, M. *Clin. Sci. Mol. Med.* **1975**, *48*, 135s.
(50) Misono, K. S.; Holladay, L. A.; Murakami, K.; Kuromizu, K.; Inagami, T. *Arch. Biochem. Biophys.* **1982**, *217*, 574.
(51) Finney, D. J. In *Probit Analysis*, 3rd ed.; Cambridge University: Cambridge, 1971; p 78.
(52) Mycek, M. In *Methods in Enzymology*; Perlmann, G., Lorand, L., Eds.; Academic: New York, 1970; Vol. XIX, p 286.

pulse sequence in which the real and imaginary parts of the t_1 dimension were collected separately by using a phase cycling scheme described by States et al.[53] Two-dimensional data sets were processed on a Vax 11/780 computer using an FT NMR computer program written by Dr. Dennis Hare.

***N*-(Benzyloxycarbonyl)-*O*-allyl-L-serine Methyl Ester (8).** To a solution of 14.0 g of *N*-(benzyloxycarbonyl)-L-serine in 300 mL of DMF cooled to ~0 °C was added 5.7 g of sodium hydride. At the end of the addition of sodium hydride, the reaction mixture was stirred at 0 °C for 20 min until hydrogen evolution stopped. Allyl bromide (5.6 mL) was added, and the reaction mixture was stirred at 0 °C for 5 min and then at room temperature for 2.5 h; 5.4 mL of methyl iodide was then added. After the mixture was stirred for an additional hour, the solid formed was filtered off and the filtrate was poured into brine (300 mL) and extracted with ether (3 × 300 mL). The combined ether extracts were washed with more brine (3 × 300 mL), then dried with anhydrous sodium sulfate, and filtered, and the solvent was evaporated in vacuo. The residual oil was purified by silica gel column chromatography (ether/hexane, 1:1), and compound **8** (8.52 g) was obtained as a colorless oil: ^{1}H NMR ($CDCl_3$) δ 3.72 (s, 3 H), 3.60–4.00 (m, 4 H), 4.30–4.60 (m, 1 H), 5.12 (s, 2 H), 5.00–6.00 (m, 4 H), 7.30 (s, 5 H). Anal. ($C_{15}H_{19}NO_5$) C, H, N.

***N*-(Benzyloxycarbonyl)-*O*-allyl-L-serinol (9).** To a solution of 285 mg of **8** in 6 mL of THF at 0 °C was added 3 mL of diisobutylaluminum hydride (1.5 M in hexane). After being stirred at 0 °C for 20 min, the reaction mixture was quenched by the addition of 1 mL of a 1 N NaOH solution. After evaporation of most of the THF, 10 mL of a 1 N sodium hydroxide solution was added and the aqueous solution was extracted with ethyl acetate (3 × 50 mL), dried with magnesium sulfate, and filtered. Evaporation of the solvent in vacuo gave the crude product as an oil, which was purified by silica gel column chromatography (ethyl acetate) to give compound **9** as a colorless oil (210 mg, 82%); ^{1}H NMR ($CDCl_3$) δ 2.55 (br m, 1 H), 3.60–3.90 (m, 5 H), 4.10 (m, 2 H), 5.10 (s, 2 H), 5.18–5.30 (m, 2 H), 5.80–5.92 (m, 1 H), 7.35–7.40 (m, 5 H). Anal. ($C_{14}H_{19}NO_4$) C, H, N.

6(*S*)-[(Benzyloxycarbonyl)amino]-4,8,10-trioxaundec-1-ene (10). To a solution of 1.7 g of **9** in 30 mL of dichloromethane at ~0 °C was added 2.82 mL of diisopropylethylamine and 1.16 mL of chloromethyl methyl ether. After 10 min, the solution was warmed to room temperature and stirred overnight. Solvent was evaporated in vacuo, and the residual oil was washed with a 10% potassium bisulfate solution, extracted with ethyl acetate (3 × 100 mL), and dried with magnesium sulfate. Filtration and evaporation of the solvent in vacuo gave the crude product, which was purified by silica gel column chromatography (ethyl acetate/hexane, 1:1) to give 1.8 g of pure **10** as a colorless oil (91%): ^{1}H NMR ($CDCl_3$) δ 3.32 (s, 3 H), 3.48–3.70 (m, 5 H), 3.98 (d, 2 H, J = 6 Hz), 4.62 (s, 2 H), 5.10 (s, 2 H), 5.15–5.30 (m, 3 H), 5.80–5.94 (m, 1 H), 7.30–7.38 (m, 5 H). Anal. ($C_{16}H_{23}NO_5$) C, H, N.

6(*S*)-[(Benzyloxycarbonyl)amino]-4,8,10-trioxaundecan-1-ol (11). To 5.0 g (16.2 mmol) of compound **10** dissolved in 40 mL of dry THF was added 66 mL of a 0.5 M solution of 9-BBN in THF at 0 °C. At the end of the addition of the 9-BBN solution, the reaction mixture was warmed to room temperature and stirred for 5 h. It was then cooled to 0 °C, and water (5 mL) was added dropwise, followed by 5.1 mL of a 3 N NaOH solution and then 5.2 mL of 30% hydrogen peroxide. The solution was warmed to 40 °C for 30 min, concentrated, washed with saturated brine, and extracted with ethyl acetate (3 × 100 mL). The organic layer was dried with anhydrous $MgSO_4$, filtered, and concentrated in vacuo. The crude product was purified by silica gel column chromatography (5% MeOH/95% CH_2Cl_2) to give 4.85 g (91%) of compound **11** as a colorless oil: ^{1}H NMR ($CDCl_3$) δ 1.78–1.86 (m, 2 H), 3.35 (s, 3 H), 3.50–3.76 (m, 8 H) 3.95–4.05 (m, 1 H), 4.60 (s, 2 H), 5.10 (s, 2 H), 5.12 (br d, 1 H), 7.32–7.40 (m, 5 H). Anal. ($C_{16}H_{25}NO_6$) C, H, N.

6(*S*)-[(Benzyloxycarbonyl)amino]-4,8,10-trioxaundecanal (12). To a solution of 0.84 mL of dimethyl sulfoxide in 9 mL of dichloromethane at −78 °C was added 0.44 mL of oxalyl chloride. After 10 min, a solution of 1.2 g of **11** in 24 mL of dichloromethane was added. The solution was stirred for 30 min, and 2.6 mL of triethylamine was added. After 5 min, the solution was washed with a 10% potassium bisulfate solution, and the aqueous solution was extracted with dichloromethane (3 × 100 mL). The combined organic solution was washed with saturated sodium bicarbonate solution and then brine, dried with anhydrous sodium sulfate, and filtered. Evaporation of the solvent in vacuo and purification of the crude product by silica gel column chromatography (ethyl acetate) gave 0.9 g of compound **12** (75%): ^{1}H NMR ($CDCl_3$) δ 2.65 (dt, 2 H, J = 2, 6 Hz), 3.32 (s, 3 H), 3.50–3.68 (m, 5 H), 3.80 (t, 2 H, J = 6 Hz), 3.92–4.00 (m, 1 H), 4.60 (s, 2 H), 5.10 (s, 2 H), 5.20 (br d, 1 H), 7.35–7.40 (m, 5 H), 9.78 (t, 1 H, J = 2 Hz). Anal. ($C_{16}H_{23}NO_6$) C, H, N.

Methyl 2(*S*)-Methyl-9(*S*)-[(benzyloxycarbonyl)amino]-3-aza-7,11,13-trioxatetradecanoate (13). To a solution of 0.9 g of compound **12** in 12 mL of 2-propanol at ~0 °C was added 0.408 g of alanine methyl ester hydrochloride and then 0.482 g of anhydrous sodium acetate. After 30 min at 0 °C, the heterogeneous solution was cooled to −20 °C and 0.22 g of sodium cyanoborohydride was added. The solution was gradually warmed to room temperature and stirred overnight. Most of the solvent was evaporated in vacuo, and the residue was dissolved in saturated sodium bicarbonate and extracted with ethyl acetate (3 × 75 mL). The combined organic phase was dried with magnesium sulfate and filtered. Evaporation of solvent in vacuo and purification of the crude product by silica gel column chromatography (5% MeOH in CH_2Cl_2) gave 1.0 g of pure compound **13** (88%): ^{1}H NMR ($CDCl_3$) δ 1.30 (d, 6 H, J = 8 Hz), 1.62–1.80 (m, 2 H), 2.60–2.72 (m, 2 H), 3.36 (s, 3 H), 3.30–3.65 (m, 5 H), 3.70 (s, 3 H), 4.60 (s, 2 H), 5.10 (s, 2 H), 5.40 (br d, 1 H), 7.20–7.30 (m, 5 H). Anal. ($C_{20}H_{32}N_2O_7$), C, H, N.

Methyl 2(*S*)-Methyl-9(*S*)-[(benzyloxycarbonyl)amino]-3-(*tert*-butyloxycarbonyl)-3-aza-7,11,13-trioxatetradecanoate (14). To a solution of 1.0 g (2.42 mmol) of compound **13** in 10 mL of chloroform was added 0.85 g (3.90 mmol) of di-*tert*-butyl dicarbonate. The solution was stirred at room temperature for 12 h, and the solvent was evaporated in vacuo. The crude product was passed through a short silica gel column (EtOAc/hexane, 1:1) to give 0.9 g (72%) of compound **14**: ^{1}H NMR ($CDCl_3$) δ 1.40 (d, 6 H, J = 8 Hz), 1.42 (s, 9 H), 3.38 (s, 3 H), 3.45–3.70 (m, 5 H), 3.65 (s, 3 H), 4.60 (s, 2 H), 5.15 (s, 2 H), 7.25 (s, 5 H). Anal. ($C_{25}H_{40}N_2O_9$) C, H, N.

Pentafluorophenyl 2(*S*)-Methyl-9(*S*)-[(benzyloxycarbonyl)amino]-3-(*tert*-butyloxycarbonyl)-3-aza-7,11,13-trioxatetradecanoate (15). To a solution of 900 mg (1.75 mmol) of compound **14** in 2 mL of water and 2 mL of dioxane was added 80 mg of lithium hydroxide. The solution was stirred at room temperature for 2 h, acidified with a 10% sodium bisulfate solution, and extracted with ethyl acetate (4 × 50 mL). The organic layer was dried with anhydrous magnesium sulfate, filtered, and concentrated to give a white solid, which was dissolved in 8 mL of ethyl acetate. The solution was cooled to 0 °C, and 360 mg of pentafluorophenol was added, followed by 396 mg of dicyclohexylcarbodiimide. The solution was stirred at 0 °C for 30 min, the white solid formed (DCU) was filtered, and the filtrate was concentrated in vacuo. The crude product was chromatographed on silica gel (EtOAc/hexane, 1:1) to give 1.10 g of compound **15** (94%): ^{1}H NMR ($CDCl_3$) δ 1.50 (s, 9 H), 1.65 (d, 6 H, J = 8 Hz), 3.35 (s, 3 H), 3.40–3.80 (m, 7 H), 4.65 (s, 2 H), 5.15 (s, 2 H), 7.40 (s, 5 H); FAB MS, (M + H) = 666.

[3*S*-(3*R,6*R**)]-Hexahydro-3-[(methoxymethoxy)methyl]-6-methyl-5-oxo-2*H*-1,4,7-oxadiazecine-7(8*H*)-carboxylic Acid 1,1-Dimethylethyl Ester (16a).** To 450 mL of dry dioxane was added 14 mL of EtOH, 210 mg of 4-pyrrolidinopyridine, and 1.0 g of 5% Pd/C. The solution was heated to 90 °C (internal temperature) while hydrogen gas was passed through continuously via a gas dispersion tube. To this solution was added a solution of 1.01 g (1.5 mmol) of compound **15** dissolved in 50 mL of dioxane over a period of 4.5 h. At this time, the bubbling of hydrogen was stopped and the solution cooled to room temperature and filtered. The filtrate was concentrated in vacuo to give a pale yellow oil, which was purified by silica gel chromatography (EtOAc) to give 460 mg of compound **16** (88%): ^{1}H NMR ($CDCl_3$) δ 1.40 (d, 3 H, J = 9 Hz), 1.50 (s,

(53) States, D. J.; Haberkorn, R. A.; Ruben, D. J. *J. Magn. Reson.* **1982**, *48*, 286.

9 H), 3.30 (s, 3 H), 3.35–3.80 (m, 7 H), 4.60 (s, 2 H). Anal. ($C_{16}H_{30}N_2O_6$) C, H, N.

[3*R*-[3*R,6*S**,7(*S**)]]-[2-[Hexahydro-3-(hydroxymethyl)-6-methyl-5-oxo-2*H*-1,4,7-oxadiazecin-7(8*H*)-yl]-2-oxo-1-(phenylmethyl)ethyl]carbamic Acid 1,1-Dimethylethyl Ester (17).** To a solution of 750 mg (2.16 mmol) of compound **16** in 20 mL of methanol was added 0.2 mL of concentrated HCl. The solution was stirred at 60 °C for 3.5 h, the solvent was removed in vacuo, and the white solid was dried overnight. The solid was dissolved in 20 mL of chloroform and 0.75 mL of triethylamine added. To this solution was added 1.05 g of Boc-Phe-NOS, and the reaction mixture was stirred at room temperature overnight. The solution was filtered, and the filtrate was concentrated to give a crude oil, which was purified by silica gel chromatography (EtOAc) to give 370 mg (30%) of compound **17**: ^{1}H NMR ($CDCl_3$) δ 0.45 (d, 3 H, J = 6 Hz), 1.45 (s, 9 H), 2.25–2.35 (m, 1 H), 2.85–3.15 (m, 6 H), 3.35–3.45 (m, 1 H), 3.60 (m, 2 H), 3.75–3.85 (m, 2 H), 4.40–4.50 (m, 2 H), 4.80 (m, 1 H), 7.20–7.35 (m, 5 H). Anal. ($C_{23}H_{35}N_3O_6$) C, H, N.

[3*S*-[3*R,6*R**,7(*R**)]]-[2-(Hexahydro-3-formyl-6-methyl-5-oxo-2*H*-1,4,7-oxadiazecin-7(8*H*)-yl)-2-oxo-1-(phenylmethyl)ethyl]carbamic Acid 1,1-Dimethylethyl Ester (18).** To a solution of 0.11 mL of oxalyl chloride in 5 mL of CH_2Cl_2 at −78 °C was added 0.22 mL of DMSO. To this solution was added 340 mg (0.75 mmol) of compound **17**. After 10 min, 0.52 mL of Et_3N was added and the solution was stirred for 15 min at −78 °C. After acidification with 10% sodium bisulfate solution, the aqueous layer was extracted with CH_2Cl_2 (3 × 50 mL), dried ($MgSO_4$), filtered, and concentrated to give a pale yellow oil, which was purified by silica gel chromatography to give 290 mg (86%) of aldehyde **18**: ^{1}H NMR ($CDCl_3$) δ 0.40 (d, 3 H, J = 6 Hz), 1.45 (s, 9 H), 2.90–3.15 (m, 5 H), 3.35–3.45 (m, 1 H), 3.60–3.65 (m, 1 H), 4.15–4.20 (m, 1 H), 4.60 (q, 1 H, J = 6 Hz), 4.80–4.85 (m, 1 H), 5.05–5.15 (m, 1 H), 5.30 (br d, 1 H), 7.20–7.35 (m, 5 H), 8.15 (br d, 1 H); MS, $M^{\bullet+}$ = 447.

[3*R*-[3*R,6*S**,7(*S**)]]-*N*-[[7-[2-[[(1,1-Dimethylethoxy)carbonyl]amino]-1-oxo-3-phenylpropyl]octahydro-6-methyl-5-oxo-2*H*-1,4,7-oxadiazecin-3-yl]methyl]-L-valine Phenylmethyl Ester (19).** To 3 mL of 2-propanol was added 100 mg (0.22 mmol) of aldehyde **18**, followed by addition of 60 mg of valine benzyl ester hydrochloride. The solution was cooled to 0 °C, and 20 mg of $NaCNBH_3$ and 40 mg of anhydrous NaOAc were added. The heterogeneous mixture was stirred at 0 °C for 2 h and at room temperature overnight. The solvent was removed in vacuo and the residue dissolved in 50 mL of chloroform and washed with saturated $NaHCO_3$. The aqueous layer was extracted with chloroform (2 × 50 mL), and the combined chloroform solution was washed with brine, dried ($MgSO_4$), and evaporated in vacuo. The crude product was purified by silica gel chromatography ($CHCl_3$/MeOH, 95:5) to give 96 mg of compound **19** (68%): ^{1}H NMR ($CDCl_3$) δ 0.36 (d, 3 H, J = 6.5 Hz), 0.88 (d, 6 H, J = 6.0 Hz), 1.45 (s, 9 H), 1.90 (heptet, 1 H, J = 6.0 Hz), 2.40–3.10 (m, 9 H), 3.30–3.35 (m, 1 H), 3.55–3.60 (m, 1 H), 3.85–3.92 (m, 1 H), 4.30–4.50 (m, 2 H), 4.70–4.80 (m, 1 H), 5.05–5.20 (AB quartet, 2 H, J = 12 Hz), 7.20–7.40 (m, 10 H); FAB MS, $(M + H)^+$ = 639.

[3*R*-[3*R,6*S**,7(*S**)]]-*N*-[*N*-[*N*-[[7-[2-[[(1,1-Dimethylethoxy)carbonyl]amino]-1-oxo-3-phenylpropyl]octahydro-6-methyl-5-oxo-2*H*-1,4,7-oxadiazecin-3-yl]methyl]-L-valyl]-L-isoleucyl]-L-histidine Methyl Ester (4).** To 5 mL of methanol containing 12 mg of 10% Pd/C was added 92 mg (0.14 mmol) of compound **19**. The heterogeneous mixture was stirred vigorously under a hydrogen atmosphere for 30 min. The catalyst was filtered, and the filtrate was concentrated in vacuo to give 73 mg of carboxylic acid. To 1.0 mL of DMF at 0 °C was added 20 mg of the carboxylic acid obtained from the hydrogenolysis, followed by 13 mg of Ile-His-OMe·2HCl, 0.011 mL of Et_3N, 7.5 mg of HOBt, and 8 mg of DCC. The solution was stirred at 0 °C for 4 h and at room temperature overnight. The solvent was removed in vacuo and the residue dissolved in EtOAc and washed with saturated $NaHCO_3$. The aqueous layer was extracted with EtOAc (2 × 25 mL) and dried ($MgSO_4$). The solvent was evaporated in vacuo to give the crude product, which was purified by silica gel chromatography (5%/MeOH/95% CH_2Cl_2) to give 12 mg (40%) of compound **4**: ^{1}H NMR ($CDCl_3$) δ 0.39 (d, 3 H, J = 7 Hz), 0.85–1.05 (m, 12 H), 1.05–1.30 (m, 2 H), 1.44 (s, 9 H), 1.45–1.80 (m, 2 H), 1.94 (m, 1 H), 2.09 (m, 1 H), 1.21 (m, 1 H), 2.50–3.22 (m, 9 H), 3.38 (m, 1 H), 3.58 (m, 1 H), 3.75 (s, 3 H), 3.77 (m, 1 H), 4.08 (m, 1 H), 4.32 (m, 1 H), 4.62 (m, 1 H), 4.78 (m, 1 H), 4.84 (m, 1 H), 5.32 (d, 1 H, J = 8.7 Hz), 6.76 (s, 1 H), 6.80 (d, 1 H, J = 6.6 Hz), 7.2–7.4 (m, 5 H), 7.47 (d, 1 H, J = 10.5 Hz), 7.57 (s, 1 H), 7.82 (d, 1 H, J = 8.1 Hz). Anal. ($C_{41}H_{64}N_8O_9\cdot H_2O$) C, H, N.

Ethyl 8(*S*)-[(Benzyloxycarbonyl)amino]-6,10,12-trioxatridec-2-enoate (20). To 40 mL of dry THF was added 1.3 mL (6.5 mmol) of triethyl phosphonoacetate. To this solution at 0 °C was added 260 mg (60% oil dispersion) of sodium hydride. The mixture was stirred at 0 °C for 5 min, and 1.0 g (3.1 mmol) of aldehyde **12** in 10 mL of THF was added. After 10 min, the reaction mixture was quenched by the addition of saturated NH_4Cl solution, extracted with etOAc (3 × 75 mL), washed with brine, and dried ($MgSO_4$) and solvent evaporated in vacuo. The crude product was purified by silica gel chromatography (hexane/EtOAc, 7:3) to give 1.06 g (87%) of compound **20**: ^{1}H NMR ($CDCl_3$) δ 1.28 (t, 3 H, J = 7 Hz), 2.45 (m, 2 H), 3.32 (s, 3 H), 3.45–3.70 (m, 6 H), 3.96 (m, 1 H), 4.18 (q, 2 H, J = 7 Hz), 4.60 (s, 2 H), 5.10 (s, 2 H), 5.15 (br d, 1 H), 5.85 (td, 1 H, J = 1, 15 Hz), 6.90 (td, 1 H, J = 6, 15 Hz). Anal. ($C_{20}H_{29}NO_7$) C, H, N.

Ethyl 8(*S*)-[(Benzyloxycarbonyl)amino]-6,10,12-trioxatridecanoate (21). To 20 mL of methanol containing 50 mg of 10% Pd/C was added 1.0 g (2.6 mmol) of compound **20**. The reaction mixture was stirred vigorously under a hydrogen atmosphere for 30 min, filtered, and concentrated. The residue was dissolved in 20 mL of CH_2Cl_2, and 600 mg (2.6 mmol) of *N*-(benzyloxy)succinimide was added. After the mixture was stirred at room temperature for 30 min, the solvent was evaporated in vacuo and the crude product was purified by silica gel chromatography (hexane/EtOAc, 7:3) to give 0.92 g (91%) of compound **21**: ^{1}H NMR ($CDCl_3$) δ 1.25 (t, 3 H, J = 7 Hz), 1.60–1.70 (m, 4 H), 2.30 (t, 2 H, J = 7.5 Hz), 3.32 (s, 3 H), 3.40–3.70 (m, 6 H), 3.95 (m, 1 H), 4.08–4.16 (q, 2 H, J = 7 Hz), 4.60 (s, 2 H), 5.10 (s, 2 H), 7.32–7.40 (m, 5 H). Anal. ($C_{20}H_{31}NO_7$) C, H, N.

8(*S*)-[(Benzyloxycarbonyl)amino]-6,10,12-trioxatridecan-1-ol (22). Using the same procedure described for the synthesis of compound **9** and starting with 900 mg (2.25 mmol) of compound **21** provided 700 mg (1.84 mmol) of compound **22** after silica gel chromatography (EtOAc): ^{1}H NMR ($CDCl_3$) δ 1.3–1.60 (m, 6 H), 3.32 (s, 3 H), 3.40–3.65 (m, 6 H), 3.92–4.00 (m, 1 H), 4.60 (s, 2 H), 5.10 (s, 2 H), 5.20 (br d, 1 H), 7.32–7.40 (m, 5 H). Anal. ($C_{18}H_{29}NO_6$) C, H, N.

8(*S*)-[(Benzyloxycarbonyl)amino]-6,10,12-trioxatridecanal (23). Via the same procedure described for the synthesis of compound **12**, 1.5 g (3.95 mmol) of alcohol **22** was oxidized to the aldehyde **23**, giving 1.35 g (3.59 mmol) of product after silica gel chromatography (hexane/EtOAc, 1:1): ^{1}H NMR ($CDCl_3$) δ 1.40–1.60 (m, 4 H), 2.60 (dt, 2 H, J = 2, 6 Hz), 3.40 (s, 3 H), 3.42–3.70 (m, 6 H), 4.05 (m, 1 H), 4.60 (s, 2 H), 5.05 (s, 2 H), 7.20 (s, 5 H), 9.60 (t, 1 H, J = 2 Hz). Anal. ($C_{18}H_{27}NO_6$) C, H, N.

[3*R*-[3*R,6*S**,7(*S**)]]-*N*-[*N*-[[7-[2-[[(1,1-Dimethylethoxy)carbonyl]amino]-1-oxo-3-phenylpropyl]-6-methyl-5-oxo-1-oxa-4,7-diazacyclododec-3-yl]methyl]-L-valyl]-L-isoleucyl]-L-histidine Methyl Ester (5).** Using the same sequence of reactions described in detail for the synthesis of compound **4**, but replacing the aldehyde **12** with the 2-carbon homologated aldehyde **23**, provided the final cyclic compound **5**: ^{1}H NMR ($CDCl_3$) (cis Phe-Ala) δ 0.60 (d, 3 H, J = 6.5 Hz), 1.44 (s, 9 H), 3.74 (s, 3 H), 6.77 (s, 1 H), 7.60 (s, 1 H); (trans Phe-Ala) δ 1.33 (s, 9 H), 3.72 (s, 3 H), 6.79 (s, 1 H), 7.62 (s, 1 H). Anal. ($C_{43}H_{68}N_8O_9\cdot H_2O$) C, H, N.

Ethyl 10(*S*)-[(Benzyloxycarbonyl)amino]-8,12,14-trioxapentadeca-2,4-dienoate (24). To 40 mL of dry THF was added 1.4 mL (6.51 mmol) of triethyl phosphonocrotonate. To this stirred solution at 0 °C was added 260 mg (60% oil dispersion) of NaH. The mixture was stirred at 0 °C for 5 min, and 1.0 g (3.1 mmol) of aldehyde **12** was added. After 10 min, the reaction mixture was quenched by the addition of saturated NH_4Cl solution, extracted with EtOAc (3 × 75 mL), washed with brine, and dried ($MgSO_4$) and solvent evaporated in vacuo. The crude product was purified by silica gel chromatography (hexane/EtOAc, 8:2) to give 810 mg (1.9 mmol) of unsaturated ester **24**: ^{1}H NMR ($CDCl_3$) δ 1.30 (t, 3 H, J = 6.5 Hz), 2.42 (q, 2 H, J = 6 Hz), 3.32 (s, 3 H), 3.45–3.60 (m, 6 H), 3.95 (m, 1 H), 4.20 (q, 2 H, J = 6.5

Hz), 4.60 (s, 2 H), 5.10 (s, 2 H), 5.80 (d, 1 H, J = 15 Hz), 6.05–6.28 (m, 2 H), 7.23 (dd, 1 H, J = 10.5, 15 Hz), 7.33–7.40 (m, 5 H). Anal. ($C_{22}H_{31}NO_7$) C, H, N.

Ethyl 10(*S*)-[(Benzyloxycarbonyl)amino]-8,12,14-trioxapentadecanoate (25). Starting with 800 mg (1.90 mmol) of unsaturated ester **24** and using the procedure described for compound **21** gave 7.50 mg (1.76 mmol) of saturated ester **25**: ^{1}H NMR ($CDCl_3$) δ 1.35 (t, 3 H, J = 7.5 Hz), 1.30–1.65 (m, 8 H), 2.30 (t, 2 H, J = 7.5 Hz), 3.32 (s, 3 H), 3.40–3.70 (m, 6 H), 3.96 (m, 1 H), 4.12 (q, 2 H, J = 7.5 Hz), 4.62 (s, 2 H), 5.10 (s, 1 H), 5.20 (br d, 1 H), 7.35–7.40 (m, 5 H). Anal. ($C_{22}H_{35}NO_7$) C, H, N.

10(*S*)-[(Benzyloxycarbonyl)amino]-8,12,14-trioxapentadecanol (26). The ester **25** was reduced with diisobutylaluminum hydride as described in the procedure for the synthesis of alcohol **9**. Starting with 1.5 g (3.52 mmol) of ester, we obtained 1.02 g (2.66 mmol) of alcohol **26** after silica gel chromatography (EtOAc): ^{1}H NMR ($CDCl_3$) δ 1.30–1.60 (br m, 10 H), 3.32 (s, 3 H), 3.40–3.70 (m, 8 H), 3.98 (br m, 1 H), 4.60 (s, 2 H), 5.10 (s, 2 H), 7.30–7.40 (m, 5 H). Anal. ($C_{20}H_{33}NO_6$) C, H, N.

10(*S*)-[(Benzyloxycarbonyl)amino]-8,12,14-trioxapentadecanal (27). Via the procedure described for the synthesis of aldehyde **12**, alcohol **26** was oxidized to the corresponding aldehyde. Starting with 1.0 g (2.6 mmol) of alcohol, we obtained 0.90 g (2.36 mmol) of aldehyde **27** after silica gel chromatography (hexane/EtOAc, 1:1): ^{1}H NMR ($CDCl_3$) δ 1.30–1.65 (m, 8 H), 2.45 (dt, 2 H, J = 2, 7.5 Hz), 3.35 (s, 3 H), 3.40–3.70 (m, 6 H), 4.60 (s, 2 H), 5.10 (s, 2 H), 7.35–7.40 (m, 5 H). Anal. ($C_{20}H_{31}NO_6$) C, H, N.

[3*R*-[3*R,6*S**,7(*S**)]]-*N*-[*N*-[*N*-[[7-[2-[[(1,1-Dimethylethoxy)carbonyl]amino]-1-oxo-3-phenylpropyl]-6-methyl-5-oxo-1-oxa-4,7-diazacyclotetradec-3-yl]methyl]-L-valyl]-L-isoleucyl]-L-histidine Methyl Ester (6).** Using the same sequence of reactions described in detail for the synthesis of compound **4**, but replacing the aldehyde **12** with the 4-carbon homologated aldehyde **27**, provided the final cyclic compound **6**: ^{1}H NMR ($CDCl_3$) (cis Phe-Ala) δ 0.60 (d, 3 H, J = 6.6 Hz), 1.42 (s, 9 H), 3.74 (s, 3 H), 6.77 (s, 1 H), 7.58 (s, 1 H); (trans Phe-Ala) δ 1.37 (d, 3 H, J = 6.6 Hz), 1.39 (s, 9 H), 3.72 (s, 3 H), 6.78 (s, 1 H), 7.60 (s, 1 H); high-resolution FAB MS, $(M + H)^+$ 869.5496 calcd for $C_{45}H_{72}N_8O_9$ = 869.5500, meas 869.5496.

Acknowledgment. We are grateful to Dr. N. S. Andreeva for providing us with her refined atomic coordinates for porcine pepsin. We also thank Drs. R. Bott and D. R. Davies for sending us their refined atomic coordinates of the pepstatin–rhizopuspepsin complex.

Registry No. 1, 105466-99-7; 2, 105467-06-9; 3, 111437-53-7; 4, 106975-94-4; 5, 111437-54-8; 6, 111437-55-9; 8, 111437-56-0; 9, 111437-57-1; 10, 111437-58-2; 11, 111437-59-3; 12, 111437-60-6; 13, 111437-61-7; 14, 111437-62-8; 15, 111437-63-9; 16a, 111437-64-0; 17, 111437-65-1; 18, 111437-66-2; 19, 111437-67-3; 19 (debenzylated), 111437-76-4; 20, 111437-68-4; 21, 111437-69-5; 22, 111437-70-8; 23, 111437-71-9; 24, 111437-72-0; 25, 111437-73-1; 26, 111437-74-2; 27, 111437-75-3; Z-Ser-OH, 1145-80-8; H-Ala-OMe·HCl, 2491-20-5; BOC-Phe-NOS, 3674-06-4; H-Val-OBzl·HCl, 2462-34-2; H-Ile-His-Ome·HCl, 109215-25-0; $(EtO)_2P(O)CH_2CO_2Et$, 867-13-0; $(EtO)_2P(O)CH_2CH{=}CHCO_2Et$, 10236-14-3; $H_2C{=}CHCH_2Br$, 106-95-6; $MeOCH_2Cl$, 107-30-2; renin, 9015-94-5.

Analgesic Dipeptide Derivatives. 4. Linear and Cyclic Analogues of the Analgesic Compounds Arginyl-2-[(*o*-nitrophenyl)sulfenyl]tryptophan and Lysyl-2-[(*o*-nitrophenyl)sulfenyl]tryptophan

M. Teresa Garcia-López,*† Rosario González-Muñiz,† M. Teresa Molinero,‡ and Joaquin Del Rio‡

Instituto de Quimica Médica, CSIC, Juan de la Cierva 3, 28006 Madrid, Spain, and Instituto Cajal, CSIC, Velázquez 144, 28006 Madrid, Spain. *Received May 1, 1987*

The syntheses of Trp(Nps)-Arg-OMe·HCl (**15**) [Trp(Nps) = 2-[(*o*-nitrophenyl)sulfenyl]tryptophan], its three stereoisomers, and their corresponding cyclic analogues are reported. The preparation of Trp(Nps)-Lys-OMe (**19**) and its cyclic analogue is also described. All these compounds have been designed as analogues of the analgesic dipeptide derivatives X-Trp(Nps)-OMe (**1b**, X = Arg; **2b**, X = Lys). In the case of dipeptides containing Arg or D-Arg, the coupling reactions were achieved via the isobutyl chloroformate and *N*-methylmorpholine mediated mixed anhydride procedure, while in the case of the Lys analogue, the *N*,*N*-dicyclohexylcarbodiimide method was employed. Sulfenylation reactions were carried out with Nps-Cl in acidic media. Cyclization to the diketopiperazines was achieved by using acetic acid as catalyst. The antinociceptive effects of all these new Trp(Nps)-containing dipeptides were evaluated after icv administration in mice, and the effects were compared with those of **1b**, **2b**, Tyr-Arg (Kyotorphin), and Tyr-D-Arg. The most active compounds, **15** and **19**, were found to exhibit a naloxone-reversible antinociceptive effect similar to those of **1b** and **2b** and approximately 50 and 12.5 times higher than those of Kyotorphin and its D isomer, respectively. Trp(Nps)-D-Arg-OMe·HCl, D-Trp(Nps)-Arg-OMe·HCl, and *cyclo*[Trp(Nps)-Arg]·HCl were also more effective than Kyotorphin (5, 10, and 10 times, respectively). In view of the structure–activity relationships obtained, several similarities between this series of Trp(Nps)-containing dipeptides and that of Kyotorphin analogues have emerged.

In previous papers,[1-3] it was reported that intracerebroventricular administration of the synthetic dipeptide derivatives arginyl-2-[(*o*-nitrophenyl)sulfenyl]tryptophan [Arg-Trp(Nps), **1a**], lysyl-2-[(*o*-nitrophenyl)sulfenyl]tryptophan [Lys-Trp(Nps), **2a**], and their corresponding methyl esters **1b** and **2b** shows a naloxone-reversible antinociceptive effect comparable with that of the enkephalin analogue D-Ala^2-Met-enkephalinamide (DAME). To date, two conclusions were obtained from structure–activity relationships: first, the need for a basic amino acid;[1,2] second, the importance of the Nps moiety, since no analgesia was found with the unsubstituted dipeptide Lys-Trp.[1] Concerning this moiety, the study of the analgesic effects of several Nps-modified analogues of **1** seems to

† Instituto de Quimica Médica.
‡ Instituto Cajal.

(1) Garicia-López, M. T.; Herranz, R.; González-Muñiz, R.; Naranjo, J. R.; De Ceballos, M. L.; Del Rio, J. *Peptides* **1986**, *7*, 39.
(2) Garcia-López, M. T.; González-Muñiz, R.; Herranz, R.; Molinero, M. T.; Del Rio, J. *Int. J. Pept. Protein Res.* **1987**, *29*, 613.
(3) Garcia-López, M. T.; González-Muñiz, R.; Molinero, M. T.; Naranjo, J. R.; Del Rio, J. *J. Med. Chem.* **1987**, *30*, 1658.

0022-2623/88/1831-0295$01.50/0